ACS OMEGA

http://pubs.acs.org/journal/acsodf

Article

Effect of the Concentration and the Type of Dispersant on the Synthesis of Copper Oxide Nanoparticles and Their Potential Antimicrobial Applications

Maribel Guzman,* Mariella Arcos, Jean Dille, Céline Rousse, Stéphane Godet, and Loïc Malet

Cite This: *ACS Omega* 2021, 6, 18576−18590

Read Online

ACCESS | Metrics & More | Article Recommendations

ABSTRACT: The bactericidal properties of copper oxide nanoparticles have growing interest due to potential application in the medical area. The present research investigates the influence of sodium dodecyl sulfate (SDS) and poly(vinylpyrrolidone) (PVP) on the production of copper oxide nanoparticles prepared from copper sulfate ($CuSO_4$) and sodium borohydride ($NaBH_4$) solutions. Different analytical techniques were used to determine the crystal nature, mean size diameter, and surface morphology of the copper oxide nanoparticles. The X-ray diffraction (XRD) patterns showed formation of nanoparticles of cuprite (Cu_2O) and tenorite (CuO) when PVP and SDS were added at the beginning of the reaction. In fact, when the Cu/PVP ratio was 1.62, Cu_2O nanoparticles were obtained. In addition, nanoparticles of CuO were synthesized when the Cu/PVP ratios were 0.54 and 0.81. On the other hand, a mixture of copper oxides (CuO and Cu_2O) and cuprite (Cu_2O) was obtained when PVP (Cu/PVP = 0.81 and 1.62) and SDS (Cu/SDS = 0.90) were added 30 min after the beginning of the reaction. Transmission electron microscopy (TEM) images show agglomerated nanoparticles with a size distribution ranging from 2 to 60 nm, while individual particles have sizes between 4.1 ± 1.9 and 41.6 ± 12.8 nm. The Kirby−Bauer method for the determination of antibacterial activity shows that small CuO (4.1 ± 1.9 nm) and Cu_2O (8.5 ± 5.3 nm) nanoparticles inhibit the growth of *Escherichia coli*, *Staphylococcus aureus MRSA*, *S. aureus* and *Pseudomonas aeruginosa* bacteria. The antibacterial test of cotton fabric impregnated with nanoparticles shows positive results. The determination of the optimal ratio of copper oxide nanoparticles per cm^2 of fabric that are able to exhibit a good antibacterial activity is ongoing.

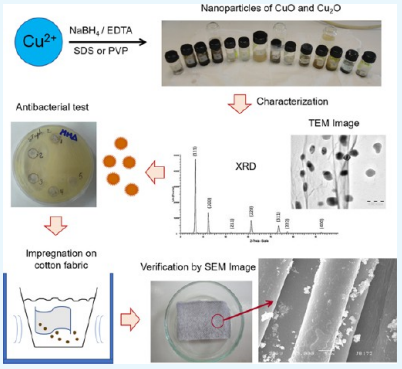

INTRODUCTION

Cuprous and cupric oxide have been investigated for decades due to their unique semiconductor and optical properties.[1] However, the study of antibacterial properties of copper oxide to develop new pharmaceutical products has gained great interest in the last few years.[2,3] In fact, cotton fibers containing copper oxide nanoparticles could be used as raw material to fabricate textiles with medical applications, such as wound dressing, protective suits, medical clothing for operation theatre or hospital areas, and others.[4]

There are several routes to obtain copper oxide nanoparticles with different shapes and sizes.[5] Some of the synthesis methods described in the literature are thermal decomposition,[6,7] calcination,[8] pyrolysis,[9] sonochemistry,[10] electrochemistry,[11−13] colloid formation,[14] microwave irradiation,[15] precipitation,[16−18] reduction,[4,19−22] reverse micelles,[23] sol−gel method,[24] self-assembled methods,[25,26] and biosynthesis using plant extracts.[27] In addition to these methods, the oxidation−reduction technique that involves a reduction of copper ions in aqueous medium using a reducing agent has been well developed.[17] Furthermore, the precipitation process is especially more attractive due to its simplicity. On the other hand, surfactants play an important role in synthesizing nanoparticles. They control the size and shape of particles and prevent their agglomeration. Dispersant molecules are likely to be adsorbed on specific crystal planes and thus promote an anisotropic growth of the crystal structure. Moreover, the presence of surfactant reduces the interfacial energy between nanoparticles and the solution, which facilitates the nucleation process and allows for its easier growth.[19] Depending on the surfactant used, it is possible to control the shape of nanoparticles by the selective binding of ligands to certain crystal facets. When ligands are used in a colloidal synthesis of nanoparticles, the interaction between them allows for self-assembly of nanoparticles in an ordered structure.[28] Many authors have reported the use of various dispersants during the synthesis of copper oxide nanoparticles,

Received: February 14, 2021
Accepted: June 24, 2021
Published: July 18, 2021

such as cetyl trimethyl ammonium bromide (CTAB),[29,30] ethylene glycol,[31] polyacrylamide (PAM),[26] poly(ethylene glycol) (PEG),[15] polyoxyethylated lauryl ether surfactant (Brij 30),[20] poly(vinylpyrrolidone) (PVP),[1,12,32−35] sodium dodecyl benzene sulfonate (SDBS),[36] sodium dodecyl sulfate (SDS),[28−30] sodium polyacrylate,[36] Triton X-100,[19,23] among others.

This study has been conducted with the purpose of investigating the influence of PVP and SDS on the mean size, morphology, and antibacterial activity of copper oxide nanoparticles synthesized by the reduction method.

RESULTS AND DISCUSSION

The effect of operational parameters, such as the type of surfactants, concentration, and addition conditions, on the synthesis of nanoparticles has been studied. In our experiment, we choose sodium dodecyl sulfate (SDS) and poly-(vinylpyrrolidone) (PVP-300 K) as surfactants. Using the method described in the Experimental Section, it was possible to synthesize copper oxide nanoparticles. By changing various parameters of the synthesis, samples with different crystalline characteristics, mean sizes, particle size distributions, and morphologies were obtained. First, the effect of SDS and PVP-300 K in the synthesis of nanoparticles was investigated. Second, the concentration of PVP-300 K was studied. Then, the effect of adding the dispersant at two different times of the synthesis (0 min and 30 min) was evaluated. Finally, we investigated whether the copper oxide nanoparticles had antibacterial activity.

Effect of Dispersant. Two and five samples, respectively, using different concentrations of SDS and PVP-300 K were synthesized (Table 1).

Table 1. Samples Prepared with Dispersant at Different Times and Concentrations[a]

	Cu/SDS		Cu/PVP	
sample	0 min	30 min	0 min	30 min
MBS01	0.90			
MDS01		0.90		
MBP01B			0.54	
MBP01			0.81	
MBP01A			1.62	
MDP01				0.81
MDP01A				1.62

[a] $[Cu^{2+}]/[NaBH_4]$ = 4:3.

The formation of CuO and Cu_2O particles from the hydrolysis of Cu^{2+} ions in aqueous media is known to be a complex process. Many reactions including cationic species have been proposed. $NaBH_4$ can reduce Cu^{2+} to form copper oxides through various redox reactions.[37] The reductant agent donates electrons to the Cu^{2+} ions. Although the reaction route and exact mechanism are not very clear, it is presumed that a series of redox reactions can develop throughout the synthesis process.

The literature reports that using sodium borohydride ($NaBH_4$), the reduction of Cu^{2+} occurs through the electron transfer from borohydride anions formed in aqueous solution. Then, nucleation of the copper atoms takes place. In this sense, three mechanisms have been proposed[38,39]

$$Cu^{2+}_{(ac)} + 2BH^-_{4(ac)} \rightarrow Cu^0_{(s)} + B_2H_{6(g)} + H_{2(g)} \quad (1)$$

$$Cu^{2+}_{(ac)} + 2BH^-_{4(ac)} + 6H_2O_{(l)} \rightarrow Cu^0_{(s)} + 2B(OH)_{3(ac)} + 7H_{2(g)} \quad (2)$$

$$4Cu^{2+}_{(ac)} + BH^-_{4(ac)} + 3H_2O_{(l)} \rightarrow 4Cu^0_{(s)} + H_3BO_{3(ac)} + 7H^+_{(ac)} \quad (3)$$

The formed copper nanoparticles could be oxidized to Cu_2O and CuO.[38,40] This oxidation reaction occurs rapidly when the copper atoms react with the dissolved oxygen molecules in the aqueous solution

$$4Cu^0_{(s)} + O_{2(g)} \rightarrow 2Cu_2O_{(s)} \quad (4)$$

$$2Cu^0_{(s)} + O_{2(g)} \rightarrow 2CuO_{(s)} \quad (5)$$

However, in the solid state, Cu_2O is slightly more stable than CuO, as indicated by their standard formation enthalpies −166.7 and −155.2 kJ/mol, respectively. This is why excess copper nanoparticles could cause the reduction of cupric oxide to cuprous oxide nanoparticles[41]

$$CuO_{(s)} + Cu_{(s)} \rightarrow Cu_2O_{(s)} \quad (6)$$

In addition, oxidation of Cu_2O can be carried out if the working pH is greater than 12.5 and the ambient temperature remains constant

$$2Cu_2O_{(s)} + O_{2(g)} \rightarrow 4CuO_{(s)} \quad (7)$$

Moreover, Cudennec et al.[42] reported that CuO could be formed through a transformation mechanism involving the generation of $Cu(OH)_2$ and, subsequently, dehydration to CuO

$$Cu^{2+}_{(ac)} + 2OH^-_{(ac)} \rightarrow Cu(OH)_{2(s)} \quad (8)$$

$$Cu(OH)_{2(s)} \rightarrow CuO_{(s)} + H_2O_{(l)} \quad (9)$$

$$Cu^{2+}_{(ac)} + DS^-_{(ac)} + 4OH^-_{(ac)} \rightarrow DS - Cu(OH)^{2-}_{4(ac)} \quad (10)$$

$$DS - Cu(OH)^{2-}_{4(ac)} \rightarrow DS - Cu(OH)_{2(s)} + 2OH^-_{(ac)} \quad (11)$$

$$DS - Cu(OH)_{2(s)} \rightarrow CuO_{(s)} + H_2O_{(l)} + 2OH^-_{(ac)} + DS^-_{(ac)} \quad (12)$$

In the presence of SDS, $Cu(OH)_2$ is stabilized and CuO is formed according to [eq 9].[28] In fact, SDS being an ionic surfactant can ionize completely in water, generating a dodecyl sulfate ion (DS^-). This ion is negatively charged and can attach to Cu^{2+} cations forming a complex ion DS-$[Cu(OH)_4]^{2-}$ according to [eq 10] and it also forms active sites to generate DS-$[Cu(OH)_2]$. Then, CuO can be produced by dehydration of $Cu(OH)_2$. Simultaneously, DS^- anions are released [eq 12].[29,32]

In addition, Shahmiri et al.[43] propose a third mechanism for the formation of CuO nanostructures that includes three stages when PVP is used

$$Cu^{2+}_{(ac)} + PVP_{(ac)} \rightarrow Cu(PVP)^{2+}_{(ac)} \quad (13)$$

https://doi.org/10.1021/acsomega.1c00818
ACS Omega 2021, 6, 18576−18590

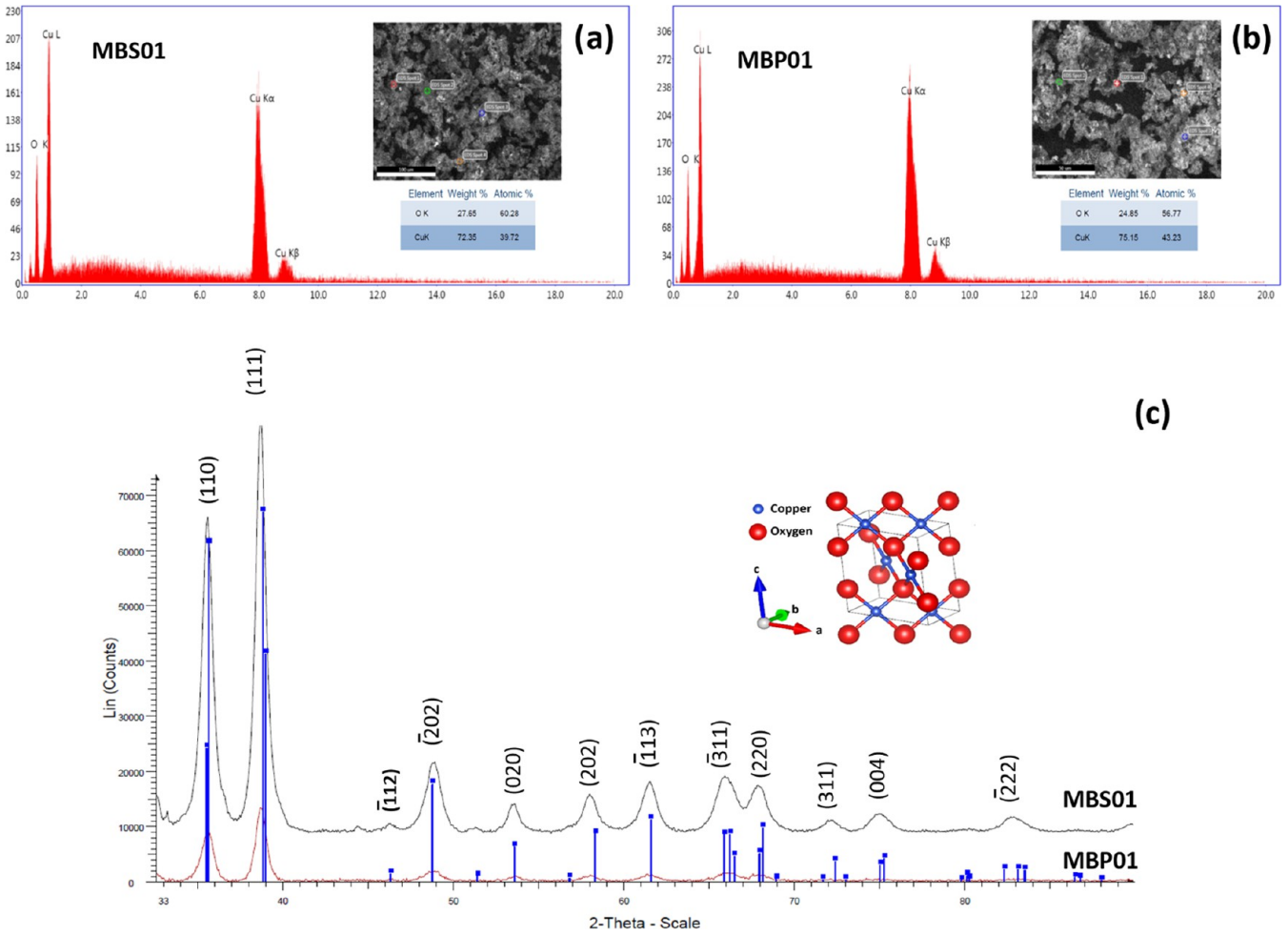

Figure 1. EDS spectrum of (a) samples MBS01 and (b) MBP01 and (c) X-ray diffraction (XRD) spectra of copper oxide nanoparticles obtained at different ratios of Cu/SDS = 0.90 (MBS01) and Cu/PVP = 0.81 (MBP01).

$$Cu(PVP)^{2+}_{(ac)} + 2OH^{-}_{(ac)} \rightarrow Cu(OH)_{2(s)}/PVP_{(ac)} \quad (14)$$

$$Cu(OH)_{2(s)}/PVP_{(ac)} \rightarrow CuO_{(s)}/PVP_{(ac)} + H_2O_{(l)} \quad (15)$$

PVP has the structure of a polyvinyl skeleton with polar groups (amide group). The amide group appears to be the most polar because they can donate and accept hydrogen bonds on both O and N atoms. The amide group donates lone-pair electrons that form a coordinative interaction with Cu^{2+} ions, thus creating a complex compound [eq 13]. PVP acts as a stabilizer for dissolved metallic salts through steric and electrostatic stabilization of the amide groups of the pyrrolidone rings. When the OH^- concentration is high enough, intense blue $Cu(OH)_2$ is formed [eq 14], indicating supersaturation due to the hydroxylation reaction. Then, a dehydration process is proposed [eq 15]. Yagi[18] and Zhang et al.[44] confirmed that it is possible to obtain Cu_2O directly with $NaBH_4$ if there is a sufficient amount of PVP in the medium.

$$4Cu^{2+}_{(ac)} + BH^{-}_{4(ac)} + 5H_2O_{(l)} \rightarrow 2Cu_2O_{(s)} + B(OH)_{3(ac)} + 2H_{2(g)} + 7H^{+}_{(ac)} \quad (16)$$

Effect of the Dispersant Nature. Copper oxide nanoparticles were obtained using SDS (Cu/SDS = 0.90) and PVP (Cu/PVP = 0.81). Energy-dispersive X-ray spectroscopy (EDS) allowed for the elemental analysis of the nanoparticles. Figure 1a,b shows the EDS spectrum of samples MBS01 (Cu/SDS = 0.90) and MBP01 (Cu/PVP = 0.81). The EDS spectra show the K and L emission peaks for copper and oxygen. No other peak belonging to any other element was detected, indicating that the as-synthesized nanoparticles did not contain impurities.

The XRD spectra of the as-prepared samples MBS01 and MBP01 show typical X-ray diffraction patterns (Figure 1c). The diffraction peaks are well indexed to those corresponding to CuO with the tenorite monoclinic structure (JCPDS card no. 00-41-254) with lattice parameters a = 4.68 Å, b = 3.42 Å, c = 5.12 Å, and β = 99.42°. Similar results were previously reported by Ganga et al.,[28] Rao et al.,[29] Reddy et al.,[30] and Siddiqui et al.[32] when SDS was used as a dispersant and also by Mayekar et al.[33] and Shahmiri et al.[43] when PVP was used as a dispersant. Further, the elemental analysis of samples MBS01 (Cu = 39.72%, O = 60.28%) and MBP01 (Cu = 43.23%, O = 56.77%) shows that the calculated atomic Cu/O ratio is 0.7 and 0.8, respectively, which is close to 1.0 (the theoretical value for CuO). In this sense, the results of EDS analysis confirm the formation of CuO determined by XRD. In this case, both SDS and PVP not only contribute to dispersion of nanoparticles but also favor the formation of CuO by immediately oxidizing all of the copper formed [eqs 1−3] to tenorite according to eq 5. In addition, if any cuprite is formed (Cu_2O), it is immediately oxidized to tenorite [eq 7]. Also,

https://doi.org/10.1021/acsomega.1c00818
ACS Omega 2021, 6, 18576−18590

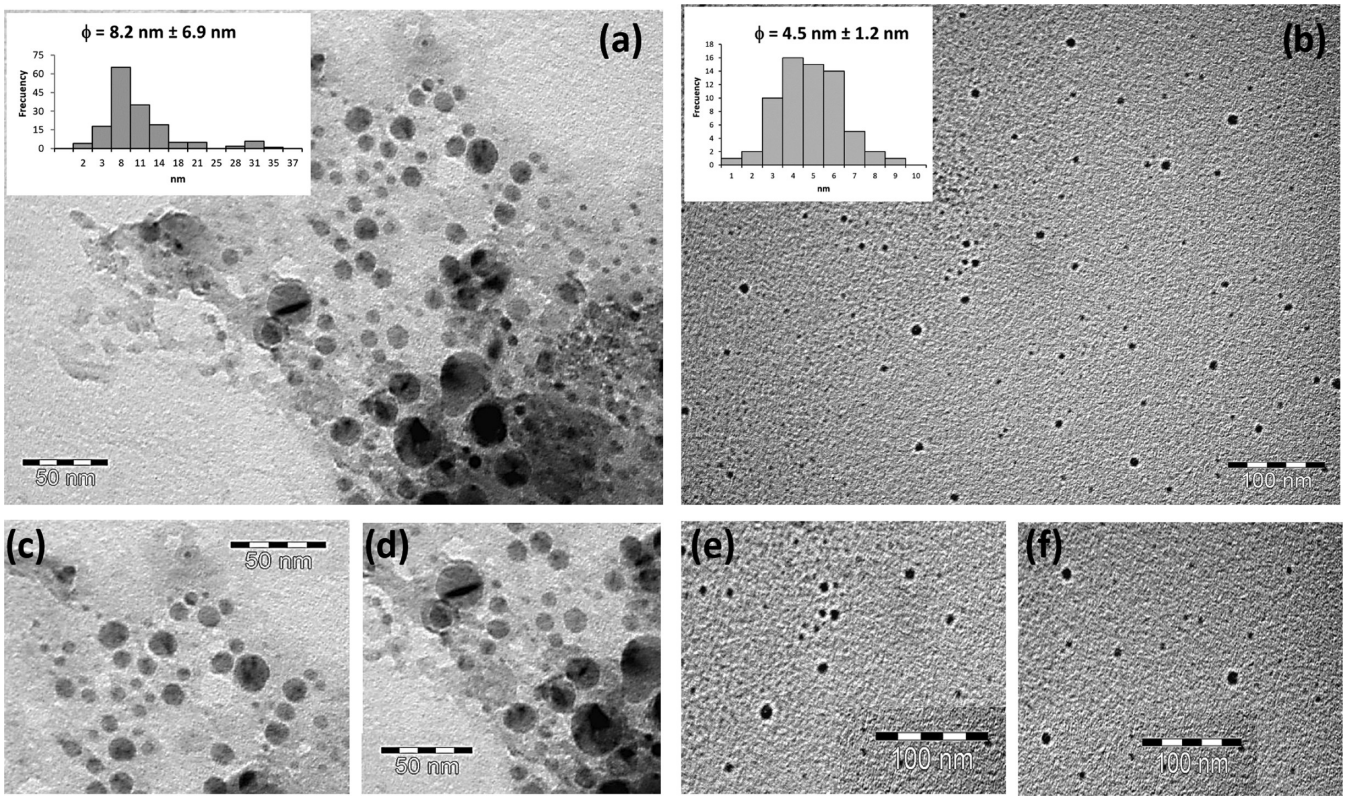

Figure 2. TEM micrographs of CuO nanoparticles prepared at different ratios of (a) Cu/SDS = 0.9 and (b) Cu/PVP = 0.81 and details of nanoparticles prepared with (c, d) SDS and (e, f) PVP.

SDS and PVP molecules stabilize $Cu(OH)_2$ for its conversion to CuO according to eqs 9 and 15, respectively.[42,43]

Through transmission electron microscopy (TEM), it was possible to analyze the morphology and size distribution of copper oxide nanoparticles. Figure 2a (sample MBS01) and Figure 2b (sample MBP01) show the presence of well-dispersed CuO nanoparticles. The TEM micrograph of sample MBS01 (Cu/SDS = 0.90) shows spherical nanoparticles when SDS is used (Figure 2c,d).

SDS can be dissolved in water, generating a negative ion (DS^-) that can attach to Cu^{2+} cations forming a complex favoring the formation of spherical CuO nanoparticles.[28] SDS is also known to be highly effective in influencing the morphology of nanoparticles through the interactions between the SDS molecule and the precursor nuclei of nanoparticles. However, excess SDS and, therefore, excess DS^- can be adsorbed on the surface of CuO nanocrystals during the transformation of $Cu(OH)_2$, inducing the formation of anisotropic branched structures. Likewise, the morphology and the size of CuO nanoparticles can be monitored if the concentration of SDS does not exceed a certain limit. In fact, diverse shapes of CuO nanostructures were obtained when different Cu/SDS ratios were used. Formation of CuO nanorods[28] (Cu/SDS = 0.1), CuO facets broken flower nanoparticles[29] (Cu/SDS = 0.2), CuO rod- and flake-shaped nanoparticles[30] (Cu/SDS = 0.6), and cubelike nanoparticles[32] (Cu/SDS = 3.7) have previously been reported.

Distribution of the nanoparticle size of sample MBS01 (Cu/SDS = 0.9) is shown in the upper left-hand corner of Figure 2a. It shows a bimodal distribution of the particle size ranging from 1.1 to 36.2 nm with a mean diameter of 8.2 ± 6.9 nm. The estimated mean diameter was determined using ImageJ software. The TEM micrograph of sample MBP01 (Cu/PVP = 0.81) is presented in Figure 2b. Figure 2e,f shows semi-spherical nanoparticles. In fact, PVP is used as a control agent that promotes preferential growth on certain specific crystal faces while obstructing others. When PVP was added into the solution, the active molecules of surfactant were adsorbed on specific crystal planes of nanocrystals because the adsorption energy of surfactant on different crystal planes is significantly different.[1] With a suitable concentration of PVP, the surfaces of CuO nanoparticles are almost covered by PVP. Then, equiaxial growth occurred, and spherical nanoparticles were obtained. However, with a similar Cu/PVP ratio, Mayekar et al.[33] (Cu/PVP = 0.75) and Shahmiri et al.[43] (Cu/PVP = 0.82) synthesized CuO nanoparticles with sheet-shaped structures were obtained. The distribution of the size of sample MBP01 shows a size distribution ranging from 0.7 to 9.5 nm with a mean diameter of 4.5 ± 1.2 nm, as illustrated in the histogram in the upper left-hand side of Figure 2b. We can observe that with similar Cu/SDS and Cu/PVP ratios, different sizes of particles were obtained. The effect of the Cu/dispersant ratio in the synthesis of nanoparticles can favor or interfere with the mechanisms involved in the formation of nanoparticles. According to LaMer et al.,[45] the nanoparticle formation mechanism has two stages: nucleation and growth.[46] The polymeric dispersant (PVP) shows a tendency to favor the nucleation step before the growth of the nuclei. In the presence of PVP, the average size of the nanoparticles may decrease because the nucleation process of CuO takes place until the critical radius is reached.

Finally, the crystallite size is calculated using the Scherrer formula from the width of the (111) plane of XRD spectra and is found to be 13.4 and 17.0 nm for samples MBS01 and

https://doi.org/10.1021/acsomega.1c00818
ACS Omega 2021, 6, 18576−18590

Table 2. Average Diameter and the Size of Crystallite Obtained for Each Sample[a]

sample	Cu/SDS	Cu/PVP	crystalline feature	mean diameter (nm)	crystallite size (nm)
MBS01	0.90[b]		CuO	8.2 ± 6.92	13.4
MDS01	0.90 (30′)		Cu_2O	8.5 ± 5.28	37.1
MBP01B		0.54[b]	CuO	11.6 ± 1.46	12.1
MBP01		0.81[b]	CuO	4.1 ± 1.93	14.9
MBP01A		1.62[b]	Cu_2O	41.6 ± 12.80	30.3
MDP01		0.81 (30′)	CuO/Cu_2O	6.0 ± 3.8	11.9
MDP01A		1.62 (30′)	CuO/Cu_2O	13.1 ± 5.5	12.6

[a]$[Cu^{2+}]/[NaBH_4]$ = 4:3. [b]Added when the reaction takes place.

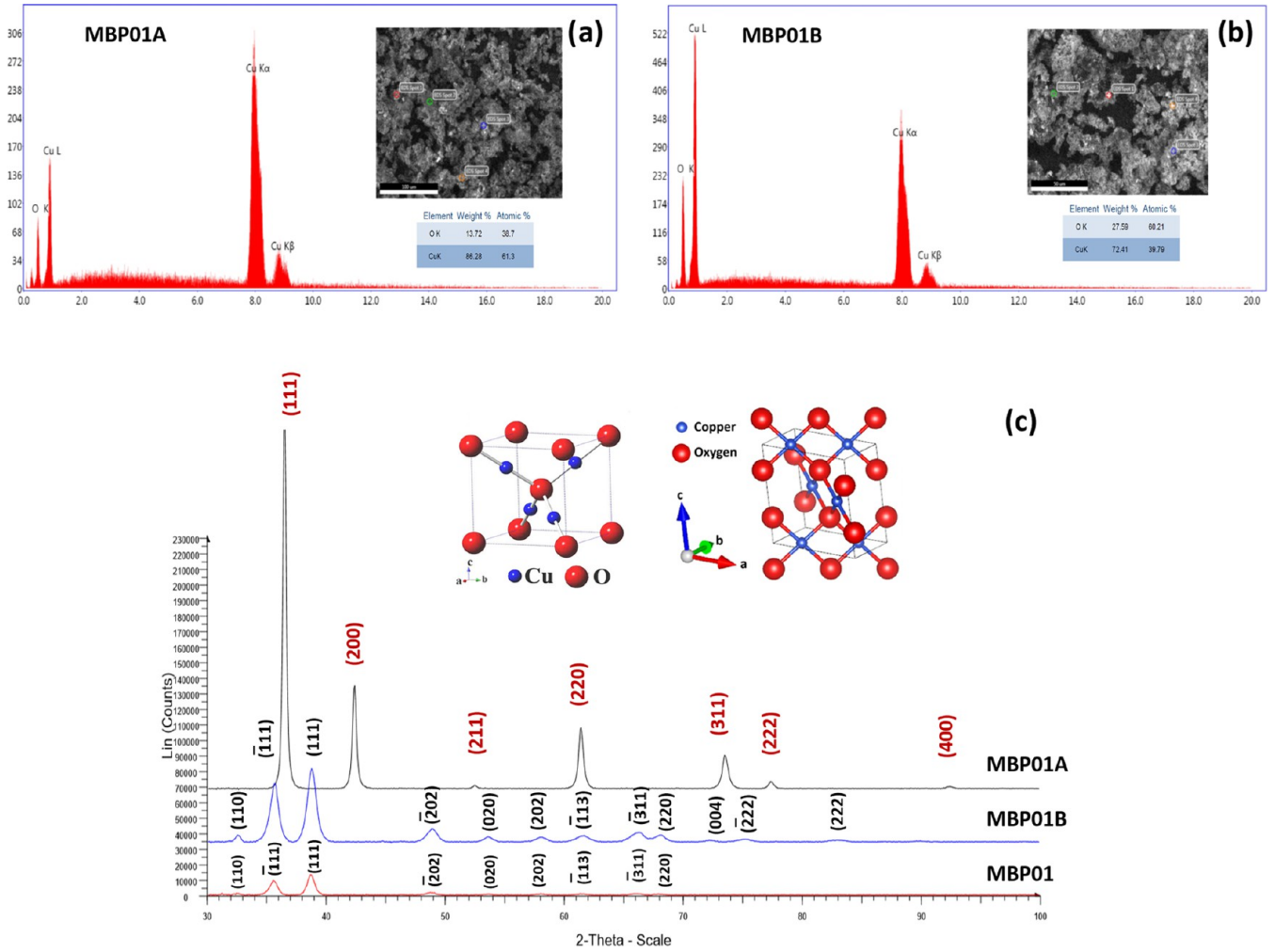

Figure 3. EDS spectrum of samples (a) MBP01A and (b) MBP01B and (c) XRD spectra of copper oxide nanoparticles prepared at different Cu/PVP ratios (1.62; 0.81; 0.54).

MBP01, respectively (Table 2). When SDS was used, similar crystallite mean diameters of 13.5 and 15.0 nm were, respectively, reported by Ganga et al.[28] and Rao et al.[29] In contrast, a bigger crystallite size of 52.1 nm was reported by Mayekar et al.[33] when PVP was employed.

Effect of the Metal/PVP Ratio. Besides the concentration of the metal precursor, the variation of the metal/PVP ratio could have a significant effect on the size and the morphology of the metal nanoparticles prepared by chemical reduction. To investigate the effect of PVP on nanoparticle synthesis, the concentration of PVP (300 000 g/mol) was varied from 3 to 10 g/L.

Figure 3a,b shows the EDS spectrum of samples MBP01A (Cu/PVP = 1.62) and MBP01B (Cu/PVP = 0.54), respectively. The K and L emission peaks for copper and oxygen are clearly observed. No other peak was detected, which implies that there were no impurities. This indicates that high-purity copper oxide nanoparticles were obtained.

Figure 3c shows the typical powder X-ray diffraction (XRD) patterns of the as-prepared samples MBP01A, MBP01, and MBP01B with addition of different concentrations of PVP (Table 1). The XRD spectrum of MBP01A exhibits interplanar distances calculated for (111), (200), (211), (220), (311), (222), and (400) that match well with the standard data. These results confirm, according to JCPDS card no. 005-0667

https://doi.org/10.1021/acsomega.1c00818
ACS Omega 2021, 6, 18576−18590

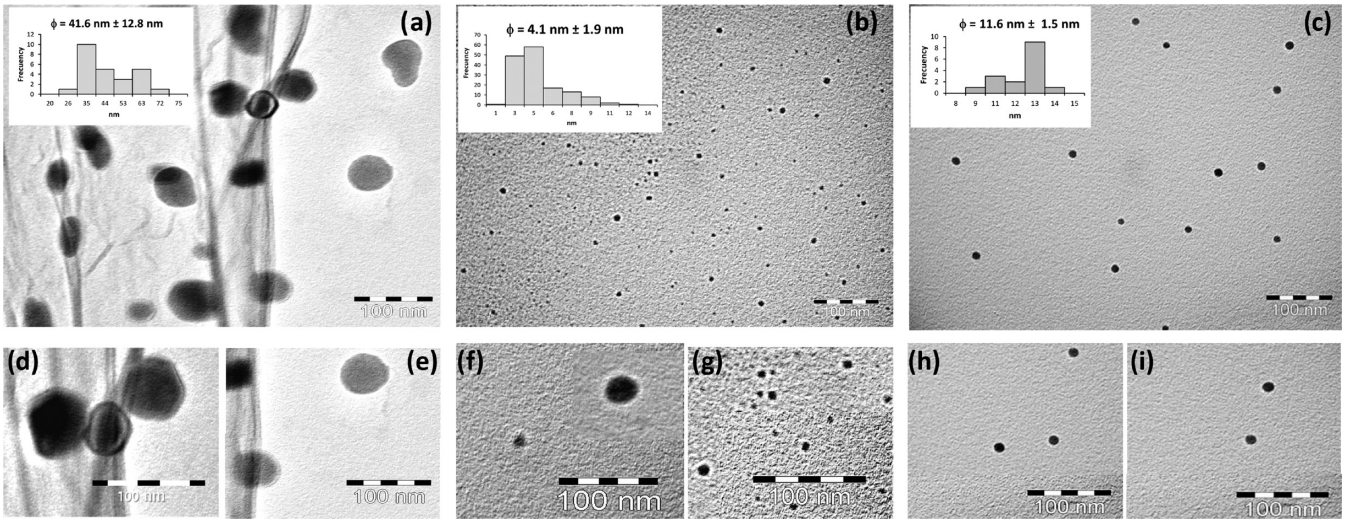

Figure 4. TEM micrographs of copper oxide nanoparticles prepared at different Cu/PVP ratios: (a) 1.62, (b) 0.81, and (c) 0.54. (d–i) Details of nanoparticles prepared with PVP at different concentrations.

(space group *Pn*3*m*, *a* = 4.23 Å), that cubic-phase cuprous oxide (Cu_2O) with a cuprite structure was obtained. This result is in agreement with those previously reported by Borgohain et al.,[12] Bai et al.,[1] Zhang et al.,[47] and Zhang et al.[34] when PVP was used as a surfactant. Furthermore, according to the EDS analysis of MBP01A (Cu = 61.3%, O = 38.7%), the calculated atomic Cu/O ratio is 1.6, which is close to the theoretical value of 2.0 for Cu_2O. Then, the results of EDS analysis confirm that Cu_2O nanoparticles were obtained, which is in agreement with the XRD results. Formation of Cu_2O can occur through several mechanisms: copper nanoparticles can be oxidized to Cu_2O [eqs 1–4], excess copper nanoparticles can oxidize cupric oxide nanoparticles to obtain cuprite [eq 6], and if the concentration of $NaBH_4$ is adequate, it is possible to reduce any possible tenorite to cuprite [eq 16].

Samples MBP01B and MBP01 show diffraction peaks that can be indexed to the phase of cupric oxide (CuO), which is in agreement with the results reported previously by Mayekar et al.[33] and Shahmiri et al.[43] In this case, both samples show typical powder diffraction patterns corresponding to a cuprite structure (JCPDS card no. 005-0667 space group *Pn*3*m*, *a* = 4.23 Å). Scherrer's formula allowed us to estimate the mean crystallite diameters, which were 30.3, 14.9, and 12.1 nm for samples MBP01A, MBP01, and MBP01B, respectively. Similar crystallite mean diameters of 45 nm for Cu_2O and 52.1 nm for CuO nanoparticles were previously reported by Borgohain et al.[12] and Mayekar et al.,[33] respectively.

As a result, two types of copper oxides were obtained using different Cu/PVP ratios. Cu_2O nanoparticles were obtained with a Cu/PVP ratio of 1.62 while nanoparticles of CuO were obtained with lower ratios (0.54 and 0.81). PVP has the structure of a polyvinyl skeleton with polar groups of oxygen and nitrogen that have pairs of free electrons to donate and form an interaction coordinated with copper ions, creating a PVP–Cu^{2+} compound [eq 13]. If the concentration of PVP is low, it is possible that the complex of PVP–Cu^{2+} could be reduced to PVP–Cu^{1+} first[48] and then copper oxide Cu^{+} (Cu_2O) can be formed. Another possibility is that PVP concentration was high enough to directly produce Cu_2O by reduction of Cu^{2+} with $NaBH_4$ according to [eq 16].[18,44] However, if the concentration of PVP increases, the CuO nanoparticles could be formed by the dehydration process according to [eq 15].

Figure 4 shows the particle size distribution of copper oxide nanoparticles when PVP was used at different concentrations. The three samples show the presence of well-dispersed copper oxide nanoparticles. The distribution of size and mean diameter for each sample is shown in the upper left-hand side of Figure 4. Figure 4a shows a distribution of the particle size ranging from 23.8 to 73.9 nm with a mean diameter of 41.6 ± 12.8 nm for Cu/PVP = 1.62 (sample MBP01A). Cu_2O nanoparticles with bigger mean diameters were previously reported by Bai et al.,[1] Zhang et al.,[34] and Zhang et al.[44] when a small Cu/PVP ratio was used (0.01–0.05). Figure 4b,c shows the distribution of the CuO nanoparticle size ranging from 8.6 to 14.6 nm with a mean diameter of 11.6 ± 1.5 nm (Cu/PVP = 0.54) and from 0.5 to 13.2 nm with a mean diameter of 4.1 ± 1.9 nm (Cu/PVP = 0.81). Details are presented in Table 2. In contrast with this result, a bigger distribution of CuO nanoparticles from 100 to 200 nm was reported by Mayekar et al.[33] when a similar Cu/PVP ratio (Cu/PVP = 0.82) was used.

TEM images show that semispherical CuO nanoparticles were obtained when Cu/PVP ratios of 0.54 and 0.81 were used. In contrast, Mayekar et al.[33] and Shahmiri et al.[43] have described the formation of CuO nanosheets when a similar ratio of Cu/PVP (0.64–0.75) and Cu/PVP (0.82) was used.

In fact, morphology, size, orientation, and dispersion of nanoparticles could be controlled by in situ polymer-assisted particle growth. The polymeric dispersant (PVP) presents the tendency to favor the nucleation step before the growth of the nuclei. In our case, the optimal molar ratio of Cu/PVP seems to be 0.81. When the Cu/PVP ratio is greater than 0.81, the average size of the copper oxide nanoparticles increases drastically, whereas when the Cu/PVP ratio is less than 0.81, the particle size increases slightly. PVP as an effective stabilizer and protecting agent can limit particle growth and prevent the particles from aggregating. But PVP can also induce the reduction of Cu^{2+} and speed up the kinetics of formation of particles [eqs 13–16], which cannot disperse as quickly as they are formed. If the concentration of PVP is high, it restrains the diffusion of the copper oxide nanoparticles. Therefore, dispersion of the nanoparticles became more difficult and

https://doi.org/10.1021/acsomega.1c00818
ACS Omega 2021, 6, 18576–18590

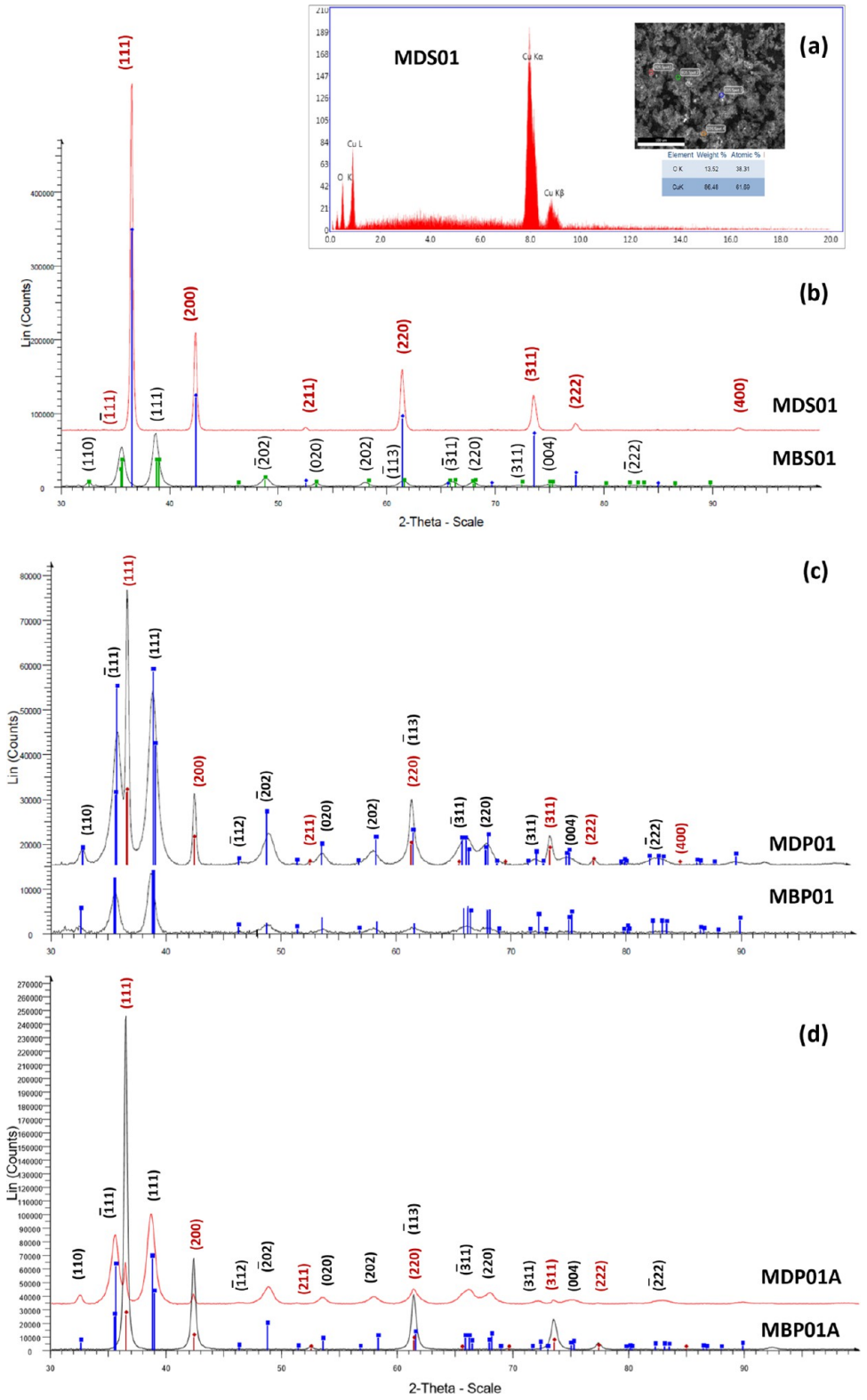

Figure 5. EDS spectrum of (a) sample MDS01 and XRD spectra of copper oxide nanoparticles prepared at different times of dispersant addition: (b) Cu/SDS = 0.9 (0 min) and 0.9 (30 min), (c) Cu/PVP = 0.81 (0 min) and 0.81 (30 min), and (d) Cu/PVP = 1.62 (0 min) and 1.62 (30 min).

aggregation occurred again, leading to an increase in the nanoparticle size. For this reason, the nanoparticles obtained with a Cu/PVP ratio of 0.54 are slightly larger than those obtained with 0.81. Details of the nanoparticles prepared with different concentrations of PVP are presented in Figure 4d–i.

In Figure 4d–i, a panoramic view of well-dispersed nanoparticles of copper oxides is presented. Figure 4d,e shows semispherical Cu_2O nanoparticles when Cu/PVP = 1.62 was used (sample MBP01A). Figure 4f–i indicates that spherical nanoparticles of CuO were obtained with Cu/PVP = 0.81 (sample MBP01) and Cu/PVP = 0.54 (sample

https://doi.org/10.1021/acsomega.1c00818
ACS Omega 2021, 6, 18576−18590

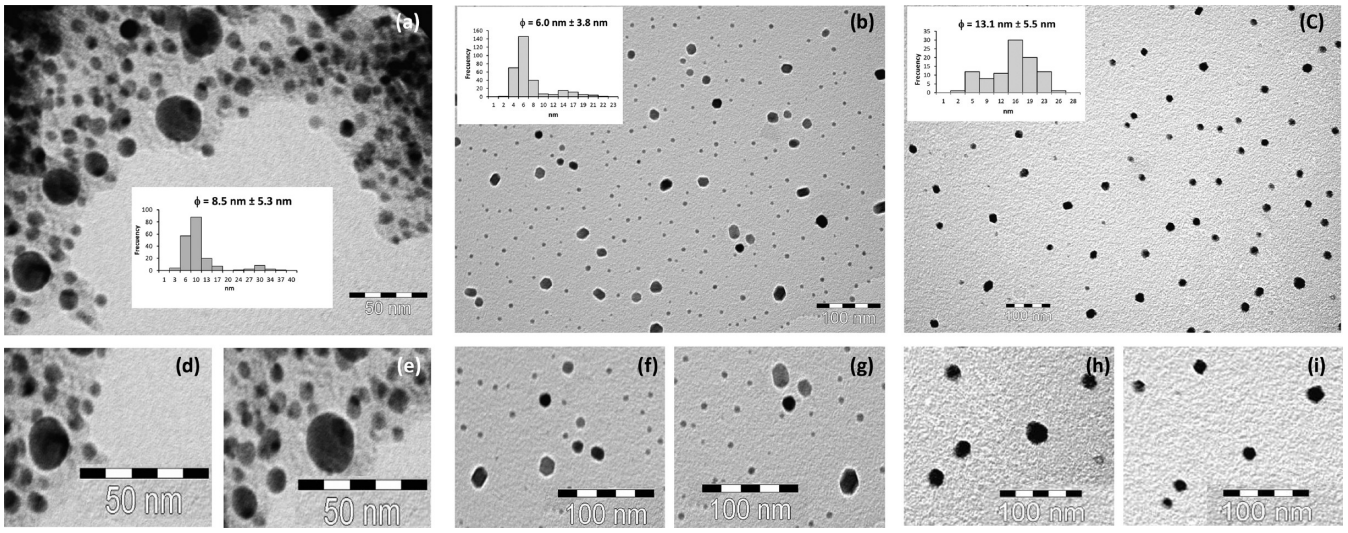

Figure 6. TEM micrographs of copper oxide nanoparticles prepared at different ratios of (a) Cu/SDS = 0.9 (30 min), (b) Cu/PVP = 1.62 (30 min), and (c) Cu/PVP = 0.81 (30 min) and details of nanoparticles prepared with (d, e) SDS and (f, i) PVP at different concentrations.

MBP01B). It is known that PVP molecules, as surfactants, play an important role in inducing the formation of nuclei and directing the growth of metal oxide crystals through selective and kinetic adsorption on the surface of particles.[16] Wu et al. reported that nonspherical nanoparticles can be obtained when PVP is used.[49] It is possible that PVP can be adsorbed on specific faces of Cu_2O, altering their growth rates, thus allowing for the generation of nonspherical shapes.

Effect of Dispersant Addition. To study the effect of dispersant addition once the synthesis had started, two samples were prepared by adding SDS and PVP 30 min after starting the reaction. Figures 1a and 5a show the EDS spectrum of samples MBS01 and MDS01 prepared with addition of SDS at 0 and 30 min of starting the reaction, respectively. Only the K and L emission peaks for copper and oxygen were observed. From the elemental analysis of MDS01 (Cu = 61.69%, O = 38.31%), the atomic Cu/O ratio can be calculated to be 1.6, which is close to the theoretical value of 2.0 for Cu_2O.

Figure 5b shows the typical powder X-ray diffraction (XRD) patterns of the as-prepared MBS01 (Cu/SDS = 0.90; 0 min) and MDS01 (Cu/SDS = 0.90; 30 min). The diffraction peaks of MBS01 show the formation of cupric oxide (CuO) with the monoclinic structure of tenorite (JCPDS card no. 00-41-254) and a = 4.68 Å, b = 3.42 Å, c = 5.12 Å, and β = 99.42° as lattice parameters. The XRD spectrum of sample MDS01 confirms that a cubic phase of cuprous oxide (Cu_2O) presenting a cuprite structure (JCPDS card no. 005-0667, space group $Pn3m$, a = 4.23 Å) was formed.

Figure 5c,d shows the XRD patterns of samples MBP01 (Cu/PVP = 0.81; 0 min), MBP01A (Cu/PVP = 1.62; 0 min), MDP01 (Cu/PVP = 0.81; 30 min), and MDP01A (Cu/PVP = 1.62; 30 min). All peaks in Figure 5c can be well indexed to the monoclinic structure of cupric oxide (CuO) (JCPDS card no. 00-41-254). However, small diffraction peaks arising from Cu_2O appear in the XRD patterns. Sample MDP01A (Figure 5d) exhibits peaks that confirm the formation of cuprous oxide (Cu_2O) with a cuprite structure (JCPDS card no. 005-0667, space group $Pn3m$, a = 4.23 Å). However, small diffraction peaks of CuO arise in the XRD patterns. Then, XRD spectra show that nanoparticles prepared with PVP added 30 min after starting the reaction are a mixture of CuO and Cu_2O. This result is in agreement with results reported previously by Liu et al.[35] In addition, the calculated atomic Cu/O ratios of MDP01 (Cu = 60.15%, O = 39.85%) and MDP01A (Cu = 61.48%, O = 38.52%) from EDS analysis were 1.51 and 1.59, which are close to theoretical values of 1.50 ($CuO{\cdot}3Cu_2O$) and 1.60 ($2CuO{\cdot}3Cu_2O$), respectively. These results confirmed that the nanopowder produced was a mixture of CuO and Cu_2O, which is in agreement with the XRD results.

The results show that when SDS is used, cuprite nanoparticles are produced, whereas when PVP is used, a mixture of copper oxide nanoparticles is obtained. During the first 30 min, there is no dispersant in the medium. Then, the reduction reaction of Cu^{2+} ions by BH_4^- is carried out, producing Cu_2O. Several possible mechanisms can be proposed. Cu nanoparticles produced [eqs 2 and 3] are subsequently oxidized to Cu_2O [according to eq 4] and CuO [according to eq 5]. In addition, some of the CuO produced can be reduced to Cu_2O by Cu nanoparticles [eq 6]. After 30 min, the added SDS is adsorbed on the surfaces of the formed nanoparticles, dispersing them without affecting the reaction mechanism. In the case of PVP addition, the remaining Cu2+ ions form CuO [eqs 13 and 15]. For this reason, a mixture of copper oxides is obtained.

Figure 6a shows well-dispersed Cu_2O nanoparticles in sample MDS01 (Cu/SDS = 0.90; 30 min). It could be presumed that stabilization of the copper oxide nanocrystals was carried out through coordinative interactions between the oxygen atoms present in SDS and on the surface of nanoparticles.[50] Figure 6a shows a bimodal distribution of the particle size ranging from 2 to 19 nm and from 22 to 39 nm. The mean diameter calculated by ImageJ was 8.5 ± 5.3 nm. In this case, semispherical nanoparticles were obtained. No significant difference in mean diameter and shape was observed when SDS was added 30 min after the reaction started.

Sample MDP01 (Cu/PVP = 0.81; 30 min) shows a bimodal particle size distribution ranging from 1.5 to 9.8 nm and from 10.0 to 22.8 nm with a mean diameter of 6.0 ± 3.8 nm (Figure 6b), while MDP01A presents particle sizes from 1.5 to 27 nm with a mean diameter of 13.1 ± 5.5 nm (Figure 6c). A similar mean diameter of sample MDP01A was reported by Liu et al.[35]

https://doi.org/10.1021/acsomega.1c00818
ACS Omega 2021, 6, 18576−18590

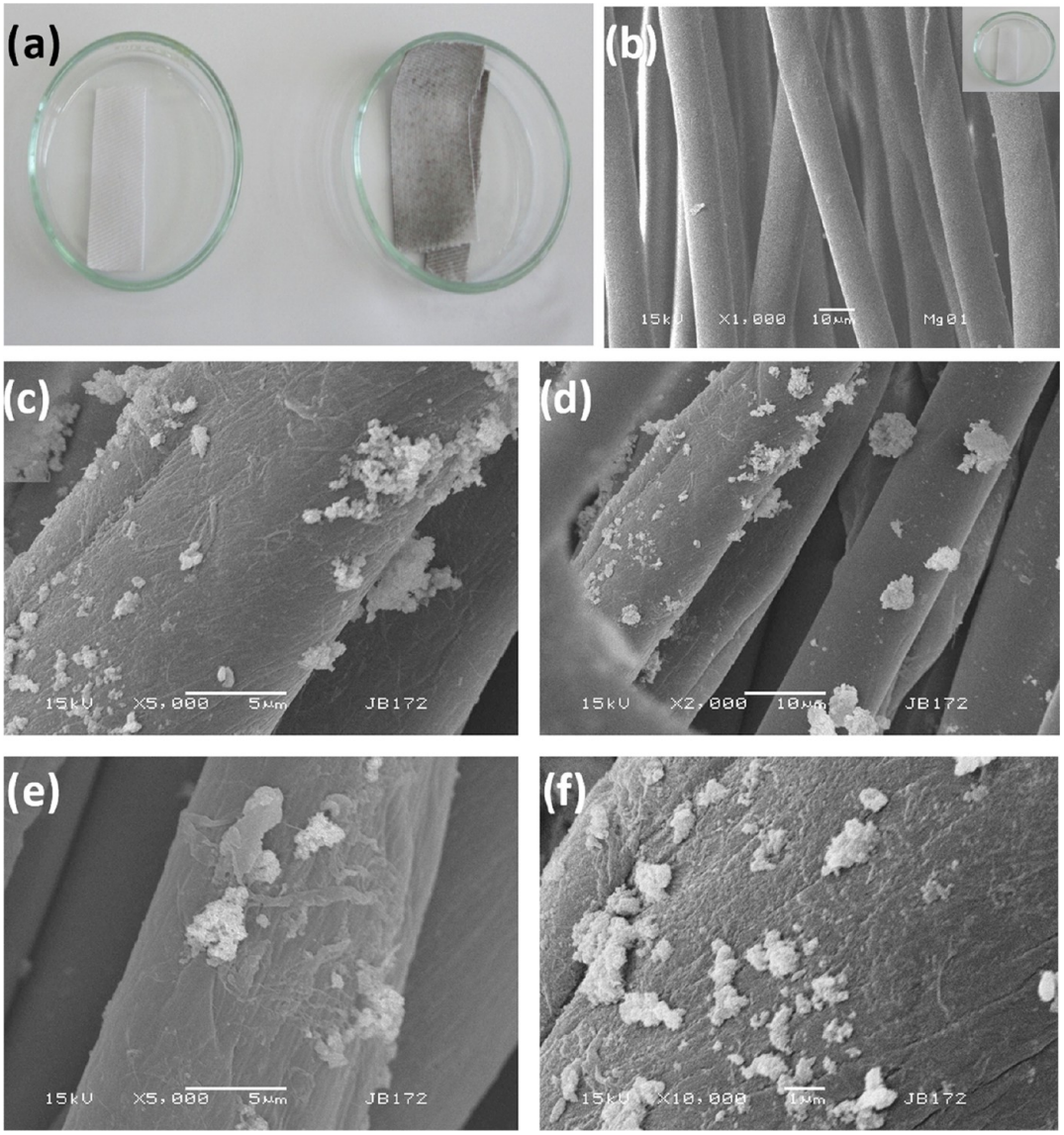

Figure 7. (a) Cotton fabric before and after nanoparticle deposition and scanning electron microscopy (SEM) images of (b) the original cotton fiber, (c) MDS01-CF, (d) MDS01-CF after washing, (e) MDP01-CF, and (f) MDP01-CF after washing.

for spherical copper oxide nanoparticles (Cu_2O and CuO). Figure 6d–i reveals the morphologies of copper oxide nanoparticles synthesized with different amounts of surfactant. By adding surfactant 30 min after the beginning of the reaction, irregular nanoparticles are observed, while spherical nanoparticles are obtained using the surfactant at the beginning of the reaction. When the Cu/PVP ratio increases from 0.81 to 1.62, the average particle size changes from 6.0 ± 3.8 to 13.1 ± 5.5 nm. The presence of PVP seems beneficial to the growth of cubes and hexagonal nanoparticles (Figure 6f–g). If the concentration of PVP increases (sample MDP01A), then all cuprous oxide surfaces are almost covered by PVP. Then, an equiaxial growth occurs, and hexagonal or semi-spherical cuprous oxide nanoparticles were obtained. If the concentration of PVP is halved (sample MDP01), only a part of the cuprous oxide surface is covered by PVP, resulting in an anisotropic growth of nanocrystals.

Table 2 summarizes the mean diameter and the crystallite size of the different samples. For the Cu/PVP = 0.81 ratio, a slight difference in nanoparticles size is observed when PVP is added at the beginning and at 30 min of the reaction. However, the difference in nanoparticle size is more evident when a smaller amount of PVP (Cu/PVP = 1.62) is added at 0 or 30 min from the start of the reaction. In fact, when PVP is added at the beginning of the reaction, particles of up to four times the size of those produced when the dispersant is added at 30 min are obtained.

Using Scherrer's formula, the crystallite diameters were determined. The values are 37.1, 11.9, and 12.6 nm for samples MDS01 (Cu/SDS = 0.90; 30 min), MDP01 (Cu/PVP = 0.81; 30 min), and MDP01A (Cu/SDS = 1.62; 30 min), respectively. A smaller crystallite mean diameter of 8 nm for a mixture of Cu_2O and CuO nanoparticles was previously reported by Liu et al.[35]

Coating Cotton Fabric. By applying ultrasonic waves, it was possible to incorporate the nanoparticles from samples MDS01 and MDP01 into cotton fabrics of approximately 11.8 cm^2 area (Figure 7a). El-Nahhal et al.[51] reported that CuO nanoparticles can be stabilized in cotton fibers thanks to the interaction of some surfactants such as SDS. In fact, the

https://doi.org/10.1021/acsomega.1c00818
ACS Omega 2021, 6, 18576−18590

Table 3. Antibacterial Activity (mm) of Copper Oxide Nanoparticle Sols against Gram-Positive and Gram-Negative Strains

sample	MBP01	MBP01B	MDS01	MBP01A	MDP01	MDP01A			
crystalline feature	CuO	CuO	Cu_2O	Cu_2O	CuO and Cu_2O	CuO and Cu_2O	raw cotton fabric	MDS01-CF	MDP01-CF
mean diameter (nm)	4.1 ± 1.9	11.6 ± 1.5	8.5 ± 5.3	41.6 ± 12.8	6.0 ± 3.8	13.1 ± 5.5			
E. coli ATCC 10536	14		18		15	12	negative	positive	positive
P. aeruginosa ATCC 10145	17		16		34	18	negative	positive	positive
S. aurus CCM 3953	19		28	15	20	17	negative	positive	positive
S. aurus MRSA ATCC 9027	22		29		23	15	negative	positive	positive

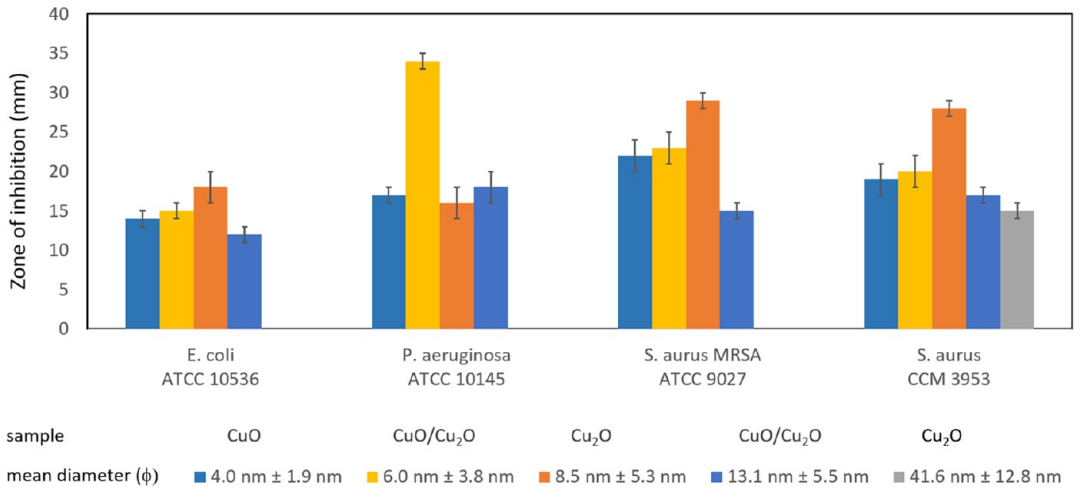

Figure 8. Results of the diffusion test of copper oxide nanoparticles against Gram-positive and Gram-negative strains.

surfactant provides better adhesion of the nanoparticles to the surface of the cotton. Indeed, the use of surfactants has improved the durability of nanoparticles and decreased their leaching. This behavior has been observed by El-Nahhal et al.[51,52] for SDS with ZnO and CuO nanoparticles.

The morphology of the fiber surface area before and after deposition of copper oxide nanoparticles was studied using SEM. Figure 7b shows the original cotton fiber before being impregnated with nanoparticles; we can observe grooves and fibrils on the surface of the fabric. SEM images of copper oxide nanoparticles covering cotton fibers are presented in Figure 7c (MDS01-CF) and Figure 7e (MDP01-CF). It is evident that it is possible to incorporate the copper oxide nanoparticles into cotton fibers when ultrasound waves are used. However, some agglomerated nanoparticles were observed. To determine if the particles would be fixed in the fabric or not, the cotton fabric was washed five times in a mini-washing machine with ultrapure water (Millipore Inc.). The copper oxide nanoparticles released into solutions were evaluated by atomic absorption spectroscopy (AAS). The tissues impregnated with ultrasound waves retain 95% (MDS01-CF) and 96% (MDP01-CF) of the copper oxide nanoparticles after having been washed five times (see Figure 7d,f). Based on this result, we can indicate that nanoparticles are strongly and physically adsorbed on the cotton surface, since these particles are not easily removed after several washes. El-Nahhal et al.[51] evaluated the stability of CuO nanoparticles incorporated into cotton fabric in the presence of SDS when 10 washing cycles was used. In our case, the 5% loss of CuO is not very significant compared to the 25% loss reported by El-Nahhal et al.[51]

Depending on their antibacterial activity, these materials can be used to design medical textiles, protective clothes and covers, and many others with the purpose of reducing the possibility of nosocomial infections.[53] Preliminary Kirby–Bauer tests show that there is some antibacterial activity (Table 3). However, further study in this field is needed.

Antibacterial Activity. The antimicrobial susceptibility of copper oxide nanoparticles against four strains was examined. To determine if a strain was susceptible, moderately or highly resistant to the synthesized nanoparticles, the Kirby–Bauer diffusion method as an antimicrobial susceptibility test was performed. For the antibacterial test, two types of strain, Gram-positives and Gram-negatives, were used as bacilli. *Staphylococcus aureus strain* (*CCM* 3953) and *S. aureus MRSA strain* (*ATCC* 9027) as Gram-positives and *Escherichia coli strain* (*ATCC* 10536) and *Pseudomonas aeruginosa strain* (*ATCC* 10145) as Gram-negative strains were used. Six samples of nanoparticles exhibiting different morphologies, average size, and chemical composition were tested. Samples MBP01 and MBP01B are tenorite and samples MDS01 and MBP01A are cuprite, while samples MDP01 and MDP01A are a mixture of copper oxides (mainly tenorite with cuprite).

In this test, disposable Petri dishes, inoculated with Gram-positive and Gram-negative bacteria at a concentration of 10^5 to 10^6 CFU/mL, were used. The disposable plate containing a specific bacterium was inoculated with the copper oxide nanoparticle sols. After 24 h of incubation at 35 °C, the inhibition zones were measured. Table 3 shows the diameters of the inhibition zones (in millimeters). The antibiotics, *vancomycin* and *gentamicin*, for Gram-positive and Gram-negative bacteria were, respectively, used as controls.

In the case of tenorite (CuO), only sample MBP01 with the smallest average size (4.1 ± 1.9 nm) shows antibacterial activity against all strains. Shahmiri et al.[43] and Naika et al.[54] reported a similar inhibition of the diameter zone against *E. coli*

https://doi.org/10.1021/acsomega.1c00818
ACS Omega 2021, 6, 18576−18590

and *S. Aurus* when CuO nanoparticles were used. In addition, a greater antibacterial susceptibility against the *S. aureus MRSA* strain was evidenced. Sample MBP01B (13.1 ± 5.5 nm) did not show positive results for any strains. For cuprite (Cu_2O), only sample MDS01 containing small nanoparticles (8.5 ± 5.3 nm) shows some antibacterial activity for all strains. In this case, the highest zones of inhibition were observed for the *S. aurus* and *S. aurus* MRSA strains. For the sample (MBP01A) with a larger nanoparticle mean size (41.6 ± 12.8 nm), antibacterial activity was observed only for the *S. aurus* strain. Instead, the two samples of the copper oxide mixture (CuO−Cu_2O) show bactericidal activity against the four strains. However, it is observed that the sample with smaller nanoparticles (6.0 ± 3.8 nm) shows a greater zone of inhibition (sample MDP01). Furthermore, the zone of inhibition for the *P. aureginosa* strain was remarkable.

Comparing the Gram-negative bacteria, we can observe that for the *E. coli* strain, the diameters of the inhibition zone are similar when samples of CuO and CuO−Cu_2O nanoparticles with close mean diameters were used (Figure 8). Azam et al.[55] reported analogous results using CuO nanoparticles with a mean size of 5 nm. For the *P. aeruginosa* strain, the best response to the antibacterial test was provided by the sample composed of both copper oxides (CuO and Cu_2O). If we compare samples with nanoparticles having similar diameters, MBP01B (CuO; 11.6 ± 1.5 nm) and MDP01A (CuO−Cu_2O; 13.1 ± 5.5 nm), we can notice that only the sample with cuprite exhibits antibacterial activity. In this case, inhibition of bacteria is enhanced due to the presence of cuprite. This effect is observed even for the larger nanoparticles. In addition, the inhibition diameters for the other samples remain almost constant. Finally, we can observe that samples MBP01, MDP01, and MDP01A show higher zones of inhibition against the *P. aeruginosa* strain than against the *E. coli* strain. Similar results were reported by Das et al.[6] when the bactericidal activity of CuO nanoparticles against these two strains was compared.

In the case of *S. aureus*, it is observed that the smallest diameter of the inhibition zone is reported for sample MBP01A, which present larger Cu_2O nanoparticles (41.6 ± 12.8 nm). The largest inhibition zone is reported for sample MDS01 (8.5 ± 5.3 nm), which suggests that small Cu_2O nanoparticles have a positive effect on bacterial inhibition.[56] Finally, we observe that for each sample, when the mean diameter of the nanoparticle decreases, the diameter of the inhibition zone increases (Table 3).

The interaction between Gram-positive bacteria and CuO and Cu_2O nanoparticles with a smaller mean size diameter seems to be stronger than the interaction with Gram-negative bacteria; this is due to the difference in cell walls between the Gram-positive and Gram-negative bacteria. Bacteria *E. coli* and *P. auriginosa* have a cell wall that is made up mainly of lipids, proteins, and lipopolysaccharides (LPSs), providing an effective shield against biocides. In contrast, Gram-positive bacteria, such as *S. aureus* and *S. aurus MRSA*, do not have LPSs in their cell wall.[57] Similar bactericidal results were previously reported when silver nanoparticles were used.[58] Therefore, the bacterial susceptibility obtained with copper oxide nanoparticles showed encouraging results. However, the MIC of each sample must still be determined.

Preliminary results suggest that copper oxide nanoparticles can be used as antimicrobial agents for the treatment of infections caused by the bacteria studied.[59] Currently, the exact bactericidal mechanism of copper oxide colloid nanoparticles on bacteria has not been identified. Certainly, there are many mechanisms that can result from the direct interaction between copper oxide nanoparticles and the outer membrane surface of bacteria. In this sense, some mechanisms have been proposed to interpret the antibacterial behavior of metal oxides.[6]

Pena et al.[60] and Kim et al.[61] have proposed different forms of action for copper oxide nanoparticles. One possibility is that the released copper ions, in an oxidation process, can intercalate with the nucleic acid strands when they interact with DNA molecules. In this way, copper ions cause a disorder of the helical structure of DNA molecules by joining them and cross-linking within and between the nucleic acid strands. Also, copper ions disrupt biochemical processes within bacterial cells.[60] Another possibility is the action of radical species that are very active. Reactive hydroxyl radicals, which are generated by copper oxides, can oxidize proteins. In this manner, by cleaving DNA and RNA molecules, lipids are oxidized, damaging their membrane.[54] Free oxygen radicals are powerful oxidizing agents. They can break down the cell wall of bacteria through a series of oxidation−reduction reactions.[61] Oxygen free radicals are generated from excited electrons on the surface of Cu_2O nanoparticles. Presently, the exact mechanism of action of CuO and Cu_2O is not known yet. The bactericidal property of nanoparticles can be associated with the mechanism of copper ions or free radical-generation species or both. Similar results of antibacterial behavior were previously reported.[11,55,56,62]

The antibacterial properties of raw cotton fabric and cotton/nanoparticles were examined against both Gram-negative and Gram-positive bacteria using the disc diffusion method (zone of inhibition test). A small inhibition halo was observed, which shows positive results. However, it is necessary to carry out more studies to determine the optimal nanoparticle dosage per cm^2 of cotton fabric. The raw cotton fabric did no show a zone of inhibition.

CONCLUSIONS

Nanoparticles of cupric and cuprous oxides with average diameters from 4.1 ± 1.9 to 41.6 ± 12.8 nm have been obtained using copper sulfate as a source of copper ions and sodium borohydride as a reducing agent. The EDS analysis confirmed the formation of copper oxide nanoparticles, since only elemental signals of copper and oxygen were observed.

We can conclude that the crystalline characteristics, particle size distribution, and the morphology of the nanoparticles change with the variation of the experimental conditions and the nature of the dispersant material used. XRD spectra confirm that tenorite nanoparticles (CuO) were obtained when SDS (Cu/SDS = 0.90; 0 min) and PVP (Cu/PVP = 0.54; 0 min and Cu/PVP = 0.81; 0 min) were used. Cuprite nanoparticles (Cu_2O) were obtained when PVP (Cu/PVP = 1.62; 0 min) and SDS (Cu/SDS = 0.90; 30 min) were used. On the other hand, a mixture of copper oxides (CuO and Cu_2O) was obtained by adding PVP at two different conditions (Cu/PVP = 0.81; 30 min and Cu/PVP = 1.62; 30 min).

TEM images show that spherical nanoparticles are obtained using SDS. In fact, it can be concluded that the morphology of nanoparticles is not affected by the use of SDS at 0 min or 30 min after the start of the reaction. However, the nanoparticle shape is affected by the use of PVP at different times of the reaction. Semispherical nanoparticles were obtained with two different Cu/PVP ratios (Cu/PVP = 0.54; 0 min and Cu/PVP

https://doi.org/10.1021/acsomega.1c00818
ACS Omega 2021, 6, 18576−18590

= 0.81; 0 min). Semispherical and hexagonal nanoparticles were obtained when PVP was added at two different times of the reaction (Cu/PVP = 1.62; 0 min and Cu/PVP = 1.62; 30 min). The influence on morphology is more evident when PVP (Cu/PVP = 0.81; 30 min) is used, since rectangular, hexagonal, and spherical nanoparticles were obtained (sample MDP01).

The influence of the dispersant on the nanoparticle size is evident when PVP is compared to SDS. The size of CuO nanoparticles decreases when the Cu/PVP ratio increases from 0.54 until 0.81. For CuO−Cu_2O nanoparticles, the mean size increased when the Cu/PVP ratio increased from 0.81 until 1.62. In this case, the amount of PVP was too low to prevent nanoparticle growth.[22]

The results of the Kirby−Bauer method demonstrated that the growth and multiplication of the *E. coli*, *P. aeruginosa*, *S. aureus*, and *S. aureus* MRSA bacteria could be inhibited by the copper oxide nanoparticles. The results show that small CuO nanoparticles have a bactericidal effect, including samples containing a small quantity of Cu_2O. Bigger nanoparticles of tenorite (CuO) do not show bacteriological activity in any case. For cuprite (Cu_2O), small nanoparticles show antibacterial activity against the four bacteria, while larger nanoparticles show only slight antibacterial activity against *S. aurus*. Based on the results obtained, we can conclude that the optimal Cu/dispersant ratios are 0.90 (Cu/SDS) and 0.81 (Cu/PVP). The nanoparticles obtained under these conditions show a higher antibacterial activity against the tested strains.

XRD revealed that CuO−Cu_2O and CuO nanoparticles coated onto cotton fibers are in the crystalline form of the monoclinic phase. The use of ultrasonic waves allows us to retain up to 96% of the nanoparticles adhering to the fabric after washing them up to five times. The minimum inhibitory concentration (MIC) using the standard microdilution method is an ongoing test. The antibacterial test performed on the cotton fabric impregnated with nanoparticles shows positive results. However, more experiments are necessary to determine the optimal ratio of copper oxide nanoparticles per cm^2 of fabric.

EXPERIMENTAL SECTION

Chemicals. Copper sulfate, $CuSO_4$ (≥98%); sodium borohydride, $NaBH_4$ (98%); ethylenediaminetetraacetic acid, EDTA, $C_{10}H_{16}N_2O_8$ (≥98%); potassium hydroxide, KOH (90%); sodium dodecyl sulfate, SDS (≥99%); and poly-(vinylpyrrolidone), PVP-300 K (99%) were purchased from Sigma-Aldrich Peru (Lima, Peru). All chemicals were of analytical purity and used as received without further purification. Milli-Q water (18 MΩ cm) was used in all experimental syntheses. The purification system (Millipore, Darmstadt, Germany) is located in our laboratory.

Bacterial Strains. The bacteria tested were *P. aeruginosa strain* (*ATCC* 10145) and *E. coli strain* (*ATCC* 10536) *as* Gram-negative strains and *S. aureus strain* (*CCM* 3953) and *S. aureus MRSA strain* (*ATCC* 9027) as Gram-positive strains. The bacteriological test was carried out at the Universidad Peruana Cayetano Heredia, Peru.

Copper Oxide Nanoparticle Synthesis. The modified chemical reduction method proposed by Badawy et al.[63] was used for the synthesis of copper oxide nanoparticles. Aqueous solutions of copper sulfate (40 mM), sodium borohydride (30 mM), potassium hydroxide (2,0 mM), ethylenediaminetetraacetic acid (EDTA, 1.0 mM), poly(vinylpyrrolidone) (PVP, 0.25−0.75% v/v), and SDS (20 mM) were used. The synthesis was carried out at room temperature. Copper sulfate solution was added to a 250 mL flask. Certain volumes of potassium hydroxide and EDTA were added. Then, using a glass burette, sodium borohydride was gradually dropped into the copper solution (at a rate of 3 mL/min). To ensure homogenization of the solutions, the reaction was carried out under magnetic stirring at room temperature. As the reaction proceeds, the light blue copper sulfate solution gradually turns into an opaque blue solution. Subsequently, the color of the solution turned reddish-brown, confirming the formation of copper oxides. After completely adding the reducing agent, the solution was stirred continuously for 30 min at room temperature. Then, the respective dispersant was added dropwise. The solution was stirred for a further 40 min. At the end of the reaction time, the nanoparticles were separated by centrifugation (12 000 rpm, 5 min) using a microcentrifuge (Eppendorf 5804). To remove excess copper ions that did not react, the nanoparticles were washed with Milli-Q water at least three times. The filtrate was kept in a desiccator. In the end, a dry copper oxide nanopowder was obtained. A similar procedure was carried out by adding the dispersant agent to the copper sulfate solution. To characterize the nanoparticles and evaluate their bacteriological activity, a certain amount of copper oxide nanopowder was suspended in deionized water using an ultrasonic cleaning container (Fisher Bioblock Scientific).

Characterization Methods for Copper Oxide Nanoparticles. *Structural Characterization.* Structural analysis was carried out using a Bruker D8 Advance X-ray diffractometer (Karlsruhe, Germany) equipped with a copper anticathode (λ Cu Kα = 1.54056 Å). XRD spectra were obtained in a range of 2θ = 30−100° using a step size of 0.03° (10 s per step as the counting time). The standard database (JCPDS) for XRD was used for phase identification. Using the information obtained from XRD patterns, the crystallite size was determined using the approximate Scherrer equation ($D = k\lambda/ß \cos\theta$). This equation describes the relationship of the crystallite size (D) considering the wavelength of the X-ray radiation (λ = 1.54056 Å), a constant related to the particle shape (k = 0.89 assuming that the particles are spherical), the line width at half maximum intensity of the most important peak (ß), and the diffraction angle (θ).

Elemental Composition Analysis. The sample chemical composition was analyzed using a scanning electron microscope (JEOL JSM 6460LA) coupled with an EDS microprobe (JEOL 1300).

Morphology Analysis. The size and morphology were obtained using transmission electron microscopy, TEM. A Philips CM20-Ultra Twin transmission electron microscope operating at 200 kV (Philips; Eindhoven, the Netherlands) was used. ImageJ software was used to elaborate the nanoparticle size distribution histograms from the TEM images. In this case, the diameters of at least 100 particles were measured. Using ultrasonic equipment, a small portion of nanopowder was dispersed in ethanol (98%) for 1 min. Then, a few drops of the copper oxide nanoparticle solutions were placed on carbon-coated TEM gold grids.

Coating Cotton Fabric. Incorporation of the copper oxide nanocrystals into cotton fibers was carried out by applying ultrasound waves. The literature reports that it is possible to use ultrasound waves to incorporate nanoparticles into textile fibers and porous materials.[64] The nanoparticles were

https://doi.org/10.1021/acsomega.1c00818
ACS Omega 2021, 6, 18576−18590

dispersed in 16 mL of Milli-Q water; to ensure a homogeneous dispersion, the vessel was exposed to ultrasonic waves for 10 min. The cotton sample (11 cm^2 approximately) was washed with Milli-Q water before being immersed in a small glass beaker containing the dispersed nanoparticles. Then, the cotton fiber was placed in this vessel. The nanoparticles and the cotton fibber sample were placed in a small ultrasonic cleaning container (Fisher Bioblock Scientific) for 30 min. Subsequently, the cotton fibber samples impregnated with the nanoparticles were washed five times and placed in a desiccator. To determine the content of copper not retained in the cotton fiber, the copper concentration in the washing solutions was analyzed using atomic absorption spectroscopy (Varian AA 220). Finally, the cotton fiber was placed in an oven (at 40 °C). The sample was placed in a desiccator for subsequent analysis using XRD and SEM.

Antibacterial Assays of Copper Oxide Nanoparticles. The disc diffusion or Kirby−Bauer method was used to evaluate the antimicrobial susceptibility of copper oxide nanoparticles.[65] After 24 h of incubation at 35 °C, the halos formed, representing the inhibition zones, were measured. Discs containing antibiotics *vancomycin* and *gentamicin* were prepared to make the necessary comparisons. The standard dilution method used to determine the minimum inhibitory concentration (MIC) required to inhibit bacterial growth is under investigation.

AUTHOR INFORMATION

Corresponding Author

Maribel Guzman − *Engineering Department, Pontifical Catholic University of Peru, Lima 32, Peru;* orcid.org/0000-0002-7954-7679; Email: mguzman@pucp.edu.pe

Authors

Mariella Arcos − *Sciences Department, Pontifical Catholic University of Peru, Lima 32, Peru*

Jean Dille − *4MAT, Université Libre de Bruxelles, B-1050 Brussels, Belgium*

Céline Rousse − *LISM, EA 4695, UFR Sciences Exactes et Naturelles, Université de Reims Champagne-Ardenne, 51687 Reims, France*

Stéphane Godet − *4MAT, Université Libre de Bruxelles, B-1050 Brussels, Belgium*

Loïc Malet − *4MAT, Université Libre de Bruxelles, B-1050 Brussels, Belgium*

Complete contact information is available at: https://pubs.acs.org/10.1021/acsomega.1c00818

Author Contributions

M.G. conceptualized the idea; proposed the methodology; supervised the project; and wrote, revised, and edited the manuscript. M.A. carried out the experiments; collected and analyzed the data; and wrote a part of the manuscript. J.D. contributed to the TEM analysis and revised and edited the manuscript. C.R. contributed to the SEM and XRD analysis and wrote a part of the manuscript. S.G. provided laboratory facilities and resources. L.M. contributed to the SEM analysis.

Notes

The authors declare no competing financial interest.

ACKNOWLEDGMENTS

Dr. M.G. thanks the Cayetano Heredia University, Perú, for the antibacterial activity carried out in the Laboratory of Biology. This work was supported by CAP 2012-0098 granted by the Pontifical Catholic University of Peru.

REFERENCES

(1) Bai, Y.; Yang, T.; Gu, Q.; Cheng, G.; Zheng, R. Shape control mechanism of cuprous oxide nanoparticles in aqueous colloidal solution. *Powder Technol.* **2012**, *227*, 35−42.

(2) (a) Ramyadevi, J.; Jeyasubramanian, K.; Marikani, A.; Rajakumar, G.; Rahuman, A. A. Synthesis and antimicrobial activity of copper nanoparticles. *Mater. Lett.* **2012**, *71*, 114−116. (b) Pal, S.; Tak, Y. K.; Song, J. M. Does the Antibacterial Activity of Silver Nanoparticles Depend on the Shape of the Nanoparticle? A Study of the Gram-Negative Bacterium *Escherichia coli*. *Appl. Environ. Microbiol* **2007**, *73*, 1712−1720.

(3) Jillani, S.; Jelani, M.; Hassan, N. U.; Ahmad, S.; Hafeez, M. Synthesis, characterization and biological studies of copper oxide nanostructures. *Mater. Res. Express* **2018**, *5*, No. 045006.

(4) (a) El-Nahhal, I. M.; Elmanama, A. A.; Amara, N. A. Synthesis of Nanometal Oxide−Coated Cotton Composites. In *Cotton Research*; Abdurakhmonov, Y. I., Ed.; IntechOpen: London, 2016; pp 279−297. (b) Rivero, P. J.; Urrutia, A.; Goicoechea, J.; Arregui, F. J. Nanomaterials for Functional Textiles and Fibers. *Nanoscale Res Lett.* **2015**, *10*, No. 501. (c) Sedighi, A.; Montazer, M.; Samadi, N. Synthesis of nano Cu_2O on cotton: Morphological, physical, biological and optical sensing characterizations. *Carbohydr. Polym.* **2014**, *110*, 489−498. (d) El-Nahhal, I. M.; Zourab, S. M.; Kodeh, F. S.; Selmane, M.; Genois, I.; Babonneau, F. Nanostructured copper oxide-cotton fibers: synthesis, characterization, and applications. *Int. Nano Lett.* **2012**, *2*, No. 14.

(5) Khodashenas, B.; Ghorbani, H. R. Synthesis of copper nanoparticles: An overview of the various methods. *Korean J. Chem. Eng.* **2014**, *31*, 1105−1109.

(6) Das, D.; Nath, B. C.; Phukon, P.; Dolui, S. K. Synthesis and evaluation of antioxidant and antibacterial behavior of CuO nanoparticles. *Colloids Surf., B* **2013**, *101*, 430−433.

(7) Salavati-Niasari, M.; Davar, F. Synthesis of copper and copper(I) oxide nanoparticles by thermal decomposition of a new precursor. *Mater. Lett.* **2009**, *63*, 441−443.

(8) Zhou, L. J.; Zou, Y. C.; Zhao, J.; Wang, P. P.; Feng, L. L.; Sun, L. W.; et al. Facile synthesis of highly stable and porous Cu_2O/CuO cubes with enhanced gas sensing properties. *Sens. Actuators, B* **2013**, *188*, 533−539.

(9) Fan, H.; Yang, L.; Hua, W.; Wu, X.; Wu, Z.; Xie, S.; Zou, B. Controlled synthesis of monodispersed CuO nanocrystals. *Nanotechnology* **2004**, *15*, 37−42.

(10) Shui, A.; Zhu, W.; Xu, L.; Qin, D.; Wang, Y. Green sonochemical synthesis of cupric and cuprous oxides nanoparticles and their optical properties. *Ceram. Int.* **2013**, *39*, 8715−8722.

(11) Jadhav, S.; Gaikwad, S.; Nimse, M.; Rajbhoj, A. Copper Oxide Nanoparticles: Synthesis, Characterization and Their Antibacterial Activity. *J. Cluster Sci.* **2011**, *22*, 121−129.

(12) Borgohain, K.; Murase, N.; Mahamuni, S. Synthesis and properties of Cu_2O quantum particles. *J. Appl. Phys.* **2002**, *92*, 1292−1297.

(13) Pandey, P.; Merwyn, S.; Agarwal, G. S.; Tripathi, B. K.; Pant, S. C. Electrochemical synthesis of multi-armed CuO nanoparticles and their remarkable bactericidal potential against waterborne bacteria. *J. Nanopart. Res.* **2012**, *14*, No. 709.

(14) (a) Dagher, S.; Haik, Y.; Ayesh, A. I.; Tit, N. Synthesis andoptical properties of colloidal CuO nanoparticles. *J. Lumin.* **2014**, *151*, 149−154. (b) Wang, Y. X.; Tang, X. F.; Yang, Z. G. A novel wet-chemical method of preparing highly monodispersed Cu_2O nanoparticles. *Colloids Surf., A* **2011**, *388*, 38−40.

(15) (a) Yang, C.; Su, X.; Wang, J.; Cao, X.; Wang, S.; Zhang, L. Facile microwave-assisted hydrothermal synthesis of varied-shaped

CuO nanoparticles and their gas sensing properties. *Sens. Actuators, B* **2013**, *185*, 159−165. (b) Wang, H.; Xu, J. Z.; Zhu, J. J.; Chen, H. Y. Preparation of CuO nanoparticles by microwave irradiation. *J. Cryst. Growth* **2002**, *244*, 88−94.

(16) Sahooli, M.; Sabbaghi, S.; Saboori, R. Synthesis and characterization of mono sized CuO nanoparticles. *Mater. Lett.* **2012**, *81*, 169−172.

(17) (a) Rangel, W. M.; Antunes, R. A.; Gracher, H. A facile method for synthesis of nanostructured copper (II) oxide by coprecipitation. *J Mater Res. Technol.* **2020**, *9*, 994−1004. (b) Phiwdang, K.; Suphankij, S.; Mekprasart, W.; Pecharapa, W. Synthesis of CuO Nanoparticles by Precipitation Method Using Different Precursors. *Energy Procedia* **2013**, *34*, 740−745. (c) El-Trass, A.; El-Shamy, H.; El-Mehasseb, I.; El-Kema, M. CuO nanoparticles: Synthesis, characterization, optical properties and interaction with amino acids. *Appl. Surf. Sci.* **2012**, *258*, 2997−3001. (d) Pike, J.; Chan, F. S. W.; Zhang, F.; Wang, X.; Hanson, J. Formation of stable Cu_2O from reduction of CuO nanoparticles. *Appl. Catal., A* **2006**, *303*, 273−277. (e) Zhu, J.; Li, D.; Chen, H.; Yang, X.; Lu, L.; Wan, X. Highly dispersed CuO nanoparticles prepared by a novel quick-precipitation method. *Mater. Lett.* **2004**, *58*, 3324−3327.

(18) Yagi, S. Potential-pH Diagrams for Oxidation-State Control of Nanoparticles Synthesized via Chemical Reduction. In *Thermodynamics - Physical Chemistry of Aqueous Systems*; Moreno-Piraján, J. S., Ed.; InTech: London, 2011; pp 223−239.

(19) Arshadi-Rastabi, S.; Moghaddam, J.; Reza, M. Synthesis, characterization and stability of Cu_2O nanoparticles produced via supersaturation method considering operational parameters effect. *J. Ind. Eng. Chem.* **2015**, *22*, 34−40.

(20) Dodoo-Arhin, D.; Leoni, M.; Scardi, P.; Garnier, E.; Mittiga, A. Synthesis, characterisation and stability of Cu_2O nanoparticles produced via reverse micelles microemulsion. *Mater. Chem. Phys.* **2010**, *122*, 602−608.

(21) Fan, G.; Li, F. Effect of sodium borohydride on growth process of controlled flower-like nanostructured Cu_2O/CuO films and their hydrophobic property. *Chem. Eng. J.* **2011**, *167*, 388−396.

(22) (a) Yuan, L.; Yin, Q.; Wang, Y.; Zhou, G. CuO reduction induced formation of CuO/Cu_2O hybrid oxides. *Chem. Phys. Lett.* **2013**, *590*, 92−96. (b) Srivastava, M.; Singh, J.; Mishra, R. K.; Ojha, A. K. Electro-optical and magnetic properties of monodispersed colloidal Cu_2O nanoparticles. *J. Alloys Compd.* **2013**, *555*, 123−130. (c) Zhu, J.; Bi, H.; Wang, Y.; Wang, X.; Yang, X.; Lu, L. Solution-phase synthesis of Cu_2O cubes using CuO as a precursor. *Mater. Lett.* **2008**, *62*, 2081−2083.

(23) Han, D.; Yang, H.; Zhu, C.; Wang, F. Controlled synthesis of CuO nanoparticles using TritonX-100-based water-in-oil reverse micelles. *Powder Technol.* **2008**, *185*, 286−290.

(24) Etefagh, R.; Azhir, E.; Shahtahmasebi, N. Synthesis of CuO nanoparticles and fabrication of nanostructural layer biosensors for detecting Aspergillus niger fungi. *Sci. Iran.* **2013**, *20*, 1055−1058.

(25) Liu, X.; Geng, B.; Du, Q.; Ma, J.; Liu, X. Temperature-controlled self-assembled synthesis of CuO, Cu_2O and Cu nanoparticles through a single-precursor route. *Mater. Sci. Eng., A* **2007**, *448*, 7−14.

(26) Lee, W.; Piao, L.; Park, C.; Lim, Y.; Do, Y.; Yoon, S.; Kim, S.-H. Facile synthesis and size control of spherical aggregates composed of Cu_2O nanoparticles. *J. Colloid Interface Sci.* **2010**, *342*, 198−201.

(27) (a) Siddiqi, K. S.; Husen, A. Current status of plant metabolite-based fabrication of copper/copper oxide nanoparticles and their applications: a review. *Biomater. Res.* **2020**, *24*, No. 11. (b) Ananda, H. C.; Desalegn, T.; Kassa, M.; Abebe, B.; Assefa, T. Synthesis of Green Copper Nanoparticles Using Medicinal Plant Hagenia abyssinica (Brace) JF. Gmel. Leaf Extract: Antimicrobial Properties. *J. Nanomater.* **2020**, 1−12. (c) Keabadile, O. P.; Aremu, A. O.; Elugoke, S. E.; Fayemi, O. E. Green and Traditional Synthesis of Copper Oxide Nanoparticles-Comparative Study. *Nanomaterials* **2020**, *10*, No. 2502.

(28) Ganga, B. G.; Santhosh, P. N. Manipulating aggregation of CuO nanoparticles: Correlation between morphology and optical properties. *J. Alloys Compd.* **2014**, *612*, 456−464.

(29) Rao, M. P.; Anandan, S.; Suresh, S.; Asiri, A. M.; Wu, J. J. Surfactant Assisted Synthesis of Copper Oxide Nanoparticles for Photocatalytic Degradation of Methylene Blue in the Presence of Visible Light. *Energy Environ. Focus* **2015**, *4*, 250−255.

(30) Reddy, S.; Kumara Swamy, B. E.; Jayadevappa, H. CuO nanoparticle sensor for the electrochemical determination of dopamine. *Electrochim. Acta* **2012**, *61*, 78−86.

(31) Namburu, P. K.; Kulkarni, D. P.; Misra, D.; Das, D. K. Viscosity of copper oxide nanoparticles dispersed in ethylene glycol and water mixture. *Exp. Therm. Fluid Sci.* **2007**, *32*, 397−402.

(32) Siddiqui, H.; Qureshi, M. S.; Haque, F. Z. Preparation of silver nanoparticles by laser ablation in polyvinylpyrrolidone solutions nanostructures and their spectroscopic analysis. *Optik* **2016**, *127*, 2740−2747.

(33) Mayekar, J.; Dhar, V.; Radha, S. Synthesis of Copper Oxide Nanoparticles Using Simple Chemical Route. *Int. J. Sci. Eng. Res.* **2014**, *5*, 928−930.

(34) Zhang, H.; Ren, X.; Chi, Z. (2007) Shape-controlled synthesis of Cu_2O nanocrystals assisted by PVP and application as catalyst for synthesis of carbon nanofibers. *J. Cryst. Growth* **2007**, *304*, 206−210.

(35) Liu, P.; Li, Z.; Cai, W.; Fang, M.; Luo, X. Fabrication of cuprous oxide nanoparticles by laser ablation in PVP aqueous solution. *RSC Adv.* **2011**, *1*, 847−851.

(36) Qiang, A.-H.; Zhao, L.-M.; Xu, C.-J.; Zhou, M. Effect of Dispersant on the Colloidal Stability of Nano-sized CuO Suspension. *J. Dispersion Sci. Technol.* **2007**, *28*, 1004−1007.

(37) (a) Liu, Q. M.; Zhou, D. B.; Yamamoto, Y.; Ichino, R.; Okido, M. Preparation of Cu nanoparticles with $NaBH_4$ by aqueous reduction method. *Trans. Nonferrous Met. Soc. China* **2012**, *22*, 117−12. (b) Lu, Y.; Wei, W.; Chen, W. Copper nanoclusters: Synthesis, characterization and properties. *Chin. Sci. Bull.* **2012**, *57*, 41−47.

(38) Zhao, H.; Yang, J.; Wang, L.; Tian, C.; Jiangaand, B.; Fu, H. Fabrication of a palladium nanoparticle/graphene nanosheet hybrid via sacrifice of a copper template and its application in catalytic oxidation of formic acid. *Chem. Commun.* **2011**, *47*, 2014−2016.

(39) (a) Fanning, J. C.; Brooks, B. C.; Hoeglund, A. B.; Pelletier, D. A.; Wadford, J. A. The reduction of nitrate and nitrite ions in basic solution with sodium borohydride in the presence of copper(II) ions. *Inorg. Chim. Acta* **2000**, *310*, 115−119. (b) Gómez-Lahoz, C.; Garcia-Herruzo, F.; Rodriguez-Maroto, J. M.; Rodriguez, J. J. Cobalt (II) removal from water by chemical reduction with sodium borohydride. *Water Res.* **1993**, *27*, 985−992.

(40) Burriel, F.; Lucena, F.; Arribas, S.; Hernández, J. Reacciones de oxido-reducción. In *Química Analítica Cuantitativa [Qualitative Analytical Chemistry]*, 18th ed.; Thomson Paraninfo: Madrid, 2006; pp 175−234.

(41) Chen, D.; Ni, S.; Fang, J. J.; Xiao, T. Preparation of Cu_2O nanoparticles in cupric chloride solutions with a simple mechano-chemical approach. *J. Alloys Compd.* **2010**, *504*, S345−S348.

(42) Cudennec, Y.; Lecerf, A. The transformation of $Cu(OH)_2$ into CuO, revisited. *Solid State Sci.* **2003**, *5*, 1471−1474.

(43) (a) Shahmiri, M.; Ibrahim, N. A.; Zainuddin, N.; Asim, N.; Bakhtyar, B.; Zaharim, A.; Sopian, K. Effect of pH on the Synthesis of CuO Nanosheets by Quick Precipitation Method. *WSEAS Trans. Environ. Dev.* **2013**, *2*, 137−146. (b) Shahmiri, M.; Ibrahim, N. A.; Shayesteh, F.; Asim, N.; Motallebi, N. Preparation of PVP-coated copper oxide nanosheets as antibacterial and antifungal agents. *J. Mater. Res.* **2013**, *28*, 3109−3118.

(44) Zhang, J.; Liu, J.; Peng, Q.; Wang, X.; Li, Y. Nearly Monodisperse Cu_2O and CuO Nanospheres: Preparation and Applications for Sensitive Gas Sensors. *Chem. Mater.* **2006**, *18*, 867−871.

(45) (a) La Mer, V. K. Nucleation in Phase Transitions. *Ind. Eng. Chem.* **1952**, *44*, 1270−1277. (b) La Mer, V. K.; Dinegar, R. H.

https://doi.org/10.1021/acsomega.1c00818
ACS Omega 2021, 6, 18576−18590

Theory, Production and Mechanism of Formation of Monodispersed Hydrosols. *J. Am. Chem. Soc.* **1950**, *72*, 4847−4854.
(46) Thanh, N. T. K.; Maclean, N.; Mahiddine, S. Mechanisms of Nucleation and Growth of Nanoparticles in Solution. *Chem. Rev.* **2014**, *114*, 7610−7630.
(47) Zhang, X.; Xie, Y.; Xu, F.; Liu, X.; Xu, D. Shape-controlled synthesis of submicro-sized cuprous oxide octahedra. *Inorg. Chem. Commun.* **2003**, *6*, 1390−1392.
(48) Guzman, A.; Arroyo, J.; Verde, L.; Rengifo, J. Synthesis and characterization of copper nanoparticles/polyvinyl chloride (Cu NPs/PVC) nanocomposites. *Procedia Mater. Sci.* **2015**, *9*, 298−304.
(49) Wu, S.; Liu, T.; Zeng, W.; He, J.; Yu, W.; Gou, Z. Rose-like Cu_2O synthesized by assisted PVP K30 hydrothermal Method. *J Mater Sci: Mater Electron.* **2013**, *24*, 2404−2409.
(50) Zhang, X.; Yin, H.; Cheng, X.; Hu, H.; Yu, Q.; Wang, A. Effects of various polyoxyethylene sorbitan monooils (Tweens) and sodium dodecyl sulfate on reflux synthesis of copper nanoparticles. *Mater. Res. Bull.* **2006**, *41*, 2041−2048.
(51) El-Nahhal, I. M.; Salem, J.; Anbar, R.; Kodeh, F. S.; Elmanama, A. Preparation and antimicrobial activity of ZnO-NPs coated cotton/starch and their functionalized ZnO-Ag/cotton and Zn(II) curcumin/cotton materials. *Sci. Rep.* **2020**, *10*, No. 5410.
(52) El-Nahhal, I. M.; Elmanama, A. A.; El Ashgar, N. A.; Amara, N.; Selmane, M.; Chehimi, M. C. Stabilization of nano-structured ZnO particles onto the surface of cotton fibers using different surfactants and their antimicrobial activity. *Ultrason. Sonochem.* **2017**, *38*, 478−487.
(53) Román, L. E.; Gomez, E. D.; Solís, J. L.; Gómez, M. M. Antibacterial Cotton Fabric Functionalized with Copper Oxide Nanoparticles. *Molecules* **2020**, *25*, No. 5802.
(54) Naika, H. R.; Lingaraju, K.; Manjunath, K.; Kumar, D.; Nagaraju, G.; Suresh, D.; Nagabhushana, H. Green synthesis of CuO nanoparticles using Gloriosa superba L. extract and their antibacterial activity. *J. Taibah Univ. Sci.* **2015**, *9*, 7−12.
(55) (a) Azam, A.; Ahmed, A. S.; Oves, M.; Khan, M. S.; Habib, S. S.; Memic, A. Antimicrobial activity of metal oxide nanoparticles against Gram-positive and Gram-negative bacteria: a comparative study. *Int. J. Nanomed.* **2012**, *7*, 6003−6009. (b) Azam, A.; Ahmed, A. S.; Oves, M.; Khan, M. S.; Habib, S. S.; Memic, A. Antimicrobial activity of metal oxide nanoparticles against Gram-positive and Gram-negative bacteria: a comparative study. *Int. J. Nanomed.* **2012**, *7*, 6003−6009.
(56) Abboud, Y.; Saffaj, T.; Chagraoui, A.; El Bouari, A.; Brouzi, K.; Tanane, O.; Ihssane, B. Biosynthesis, characterization and antimicrobial activity of copper oxide nanoparticles (CONPs) produced using brown alga extract (*Bifurcaria bifurcata*). *Appl. Nanosci.* **2014**, *4*, 571−576.
(57) Speranza, G.; Gottardi, G.; Pederzolli, C.; Lunelli, L.; Canteri, R.; Pasquardini, L. Role of chemical interactions in bacterial adhesion to polymer surfaces. *Biomaterials* **2004**, *25*, 2029−2037.
(58) Guzman, M.; Dille, J.; Godet, S. Synthesis and antibacterial activity of silver nanoparticles against gram-positive and gram-negative bacteria. *Nanomedicine* **2012**, *8*, 37−45.
(59) (a) Rai, V. R.; Bai, A. J. Nanoparticles and Their Potential Application as Antimicrobials, Science against Microbial Pathogens: Communicating Current Research and Technological Advances. In *Microbiology Series*; Méndez-Vilas, A., Ed.; Formatex: Madrid, 2011; pp 197−209. (b) Ren, G.; Hu, D.; Cheng, E.; Vargas-Reus, M. A.; Reip, P.; Allaker, R. P. Characterisation of copper oxide nanoparticles for antimicrobial applications. *Int. J. Antimicrob. Agents* **2009**, *33*, 587−590.
(60) Pena, M. M. O.; Koch, K. A.; Thiele, D. J. Dynamic regulation of copper uptake and detoxification genes in Saccharomyces cerevisiae. *Mol. Cell. Biol.* **1998**, *18*, 2514−2523.
(61) Kim, J. H.; Cho, H.; Ryu, S. E.; Choi, M. U. Effects of metals ions on the activity of protein tyrosine phosphate VHR: Highly potent and reversible oxidative inactivation by Cu_2O ion. *Arch. Biochem. Biophys.* **2000**, *382*, 72−80.
(62) Guzman, M.; Arcos, M.; Dille, J.; Godet, S.; Rousse, C. Effect of the Concentration of $NaBH_4$ and N_2H_4 as Reductant Agent on the Synthesis of Copper Oxide Nanoparticles and its Potential Antimicrobial Applications. *Nano Biomed. Eng.* **2018**, *10*, 392−405.
(63) Badawy, S.-M.; El-Khashab, R.-A.; Nayl, A.-A. Synthesis, Characterization and Catalytic Activity of Cu/Cu_2O Nanoparticles Prepared in Aqueous Medium. *Bull. Chem. React. Eng. Catal.* **2015**, *10*, 169−174.
(64) (a) Perelshtein, I.; Perkas, N.; Gedanken, A. *Ultrasonic Coating of Textiles by Antibacterial and Antibiofilm Nanoparticles. In Handbook of Ultrasonics and Sonochemistry*; Ashokkumar, M. Ed.; Springer: Singapore, 2015; pp 1−27. (b) Abramova, A. V.; Abramov, V. O.; Gedanken, A.; Perelshtein, I.; Bayazitov, V. M. An ultrasonic technology for production of antibacterial nanomaterials and their coating on textiles. *Beilstein J Nanotechnol.* **2014**, *5*, 532−536. (c) Ma, J.; Chen, S.; Liu, C.; Xu, W.; Wang, S. The influences of ultrasonic on embedding nanoparticles into porous fabric materials. *Appl. Acoust.* **2008**, *69*, 763−769.
(65) Clinical and Laboratory Standards Institute. *Performance Standards for Antimicrobial Disk and Dilution Susceptibility Test: M2-A9. Performance Standards for Antimicrobial Susceptibility Testing. 18th Informational Supplement: M100-S18*, 2008.

https://doi.org/10.1021/acsomega.1c00818
ACS Omega 2021, 6, 18576−18590